J.Soil Sci. and Agric. Eng., Mansoura Univ., Vol. 9 (5): 229- 236, 2018

Predicting Agricultural Potentiality using Land Degradation Factors in East of Rosetta Branch, Nile Delta, Egypt

Abuzaid, A. S.[1]; M. A. Bassouny[1] and A. D. Abdellatif[2]
[1] Soil and Water Department, Faculty of Agriculture, Benha University, Egypt
[2] Soil, Water and Environment Research Institute, Agricultural Research Center, Egypt

ABSTRACT

The Nile Delta is the backbone of agriculture in Egypt and undergoes land degradation, thus predicting land performance is of great concern. Chemical and physical processes and risks of degradation were evaluated for 887.09 km2 (88709 ha) in Kafr El-Sheikh Governorate, along the eastern bank of the Nile River (Rosetta branch). The revised Storie index and the Applied System for Land Evaluation (ASLE) were used to calculate land productivity index (LPI) and land capability index (LCI), respectively. Twenty soil profiles were dug to a depth of 150 cm. The multiple linear regression (MLR) was operated to predict LPI and LCI based on land degradation factors (LDF) including EC, ESP, bulk density, depth, slope, silt, and clay. Based on Landsat 8 satellite imagery and digital elevation model (DEM), the main landforms include levee, overflow mantle, recent terraces, middle terraces and old terraces. The area was affected by slight to moderate salinity hazards, slight to severe sodicity hazards, and moderate to extreme compaction hazards due to Mediterranean seawater intrusion besides mismanagement practices. The area was affected by low chemical degradation risks, but moderate to very high physical risks. The LP ranged from good to poor, while LC was good to fair. The MLR models showed high accuracy when predicting LPI and LCI based on EC, ESP, bulk density, silt, and clay. The models would be effective to verify the impacts of LDF on land's agricultural potential.

Keywords: Land degradation, Land productivity, Land capability, Regression, North Nile Delta

INTRODUCTION

Land degradation (LD) is a temporary or permanent decline in the productive capacity and quality of land, causing a decrease in its ecological and economic functions. It is one of the world's greatest challenges, especially for the developing countries in Asia and Africa (Mahala, 2017). It affects over 1.5 billion people worldwide since about 12 million hectares of arable lands are lost every year (Safriel, 2017). Drylands are sensitive to LD and occupy over 41% of the world land surfaces, and house nearly 35% of the global population (Ravi *et al.*, 2010). Almost 90% of the drylands are in the developing countries, where LD costs 4-8% of the national Gross Domestic Product (GDP) (D'Odorico *et al.*, 2013). Africa houses nearly 73% of the drylands and LD affects about 268 million people (Mganga *et al.*, 2018).

In Egypt, the severity of LD is complicated since agriculture plays a vital role in the national economy, accounting for 14.5% of the GDP, 30% of the total foreign exchange earnings, and 41% of the workforce (Abdel Meguid, 2017). The total cultivated area is 3.6 million hectares, making 4% of Egypt's total area (Zohry and Ouda, 2018). With a growing population of an annual rate of 1.84%, changing food diets, and competition of arable land and other activities, this small portion is no longer enough to supply food demand (Said *et al.*, 2016).

Arable land in the Nile Delta is 1.85 million hectares that represent 51.2% of the total cultivated land, and 73.3% of the old fertile alluvial soils in Egypt. This region houses half of Egypt's inhabitants and about two-thirds of the agricultural activities (Mohamed, 2017a). Fertile lands in this region undergo degradation processes including salinization, sodification, water logging, compaction (AbdelRahman *et al.*, 2017), chemical and physical risks (ElBaroudy and Moghanm, 2014), and water erosion due to Mediterranean Sea level rise, in particular along the promontories of the Rosetta and Damietta branches (Embabi, 2018).

From the agricultural point of view, land is usually evaluated in terms of productivity and capability. The former refers the ability to output optimum yields under a standard set of management practices, while the latter indicates the potential of a land to be used for agriculture or other uses according to the degree of limitations (Blume *et al.*, 2016). The Storie index is an accepted parametric method for rating soil productivity. The first version appeared in 1933, and the last update was in 1978 (Blume *et al.*, 2016). A revised version was developed by the University of California, Division of Agriculture and Natural Resources. The ratings in the revised version are generated digitally from the USDA Natural Resource Conservation Services (NRCS) National Soil Information System (NSIS), providing an easy-applicable model (O'geen *et al.*, 2008). The Applied System for Land Evaluation (ASLE) software, developed by Ismail *et al.* (2001), is used to assess land capability in arid and semi-arid regions. The main goals of the current study were to (i) assess land degradation status and risks, (ii) appraise land productivity and land capability, and (iii) develop mathematical models to predict LPI and LCI based on LDF.

MATERIALS AND METHODS

Site description

The studied area is located in Kafr El-Sheikh Governorate, north Nile Delta, Egypt, between 30° 25′ 34″ to 30° 54′ 64″ E and 31° 01′ 30″ and 31° 25′ 05″ N (Fig. 1). It covers 887.09 km^2 (88709 ha) along the eastern bank of the Nile River (Rosetta branch). The area is composed of sedimentary sequences deposited between Oligocene and Pliocene/Pleistocene extending to recent times (Mohamed, 2017a). The area is dominated by a Mediterranean climate (EMA, 2011) with a hot arid summer and a little rain in winter. The minimum temperature is 6.7 °C in February, and the maximum is 33.4 °C in June. The total annual rainfall is 76 mm. The potential evapotranspiration (PET) is 4.85 mm day^{-1}. The soil temperature regime is Thermic and soil moisture regime is Torric (Soil Survey Staff, 2014a). The crop pattern is dominated by field crops (91.9%), including wheat, rice, sugar beet, clover, cotton and maize. The remaining area is occupied by vegetable

crops (7.8%); onion, tomato, and potato, and fruit crops (1.3%); guava, fig, and date palm (Zohry and Ouda, 2018).

Fig. 1. Location map of the studied area

Geomorphic units

The area is covered by one Landsat-8 operational land imager (OLI) scene (path 177, row 38 and 28.5 m spatial resolution). ENVI 5.1 software was used for digital image processing. An unsupervised classification (ISO DATA classifier) was performed. Supervised classification (maximum likelihood) was then executed to relate the various clusters to meaningful ground categories. Topographic maps with a scale of 1:50,000 covering the area (Egyptian General Survey Authority) were converted to a digital format. Contour lines and spot heights were digitized within ArcGIS software 10.2.2 to generate a digital elevation model (DEM) by means of interpolation. By integrating the processed OLI image and DEM, the geomorphic units were extracted according to Zinck and Valenzuela (1990).

Field work and laboratory analysis

Twenty soil profiles were dug in the studied area (Fig.2) to a depth of 150 cm and were described according to FAO (2006). Disturbed and undisturbed soil samples were collected for laboratory analyses. Chemical (pH, electrical conductivity, cation exchange capacity, exchangeable sodium percentage, organic matter, calcium carbonate, and gypsum) physical (particle size distribution, bulk density, available water content and hydraulic conductivity) analyses were performed following the standard methods of Soil Survey Staff (2014b).

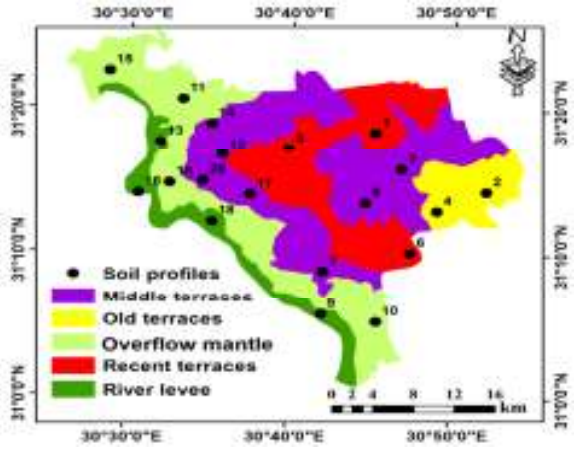

Fig. 2. Geomorphic units and locations of soils profiles in the studied area

Assessment of land degradation

The global assessment of soil degradation (GLASOD) model (FAO, 1980) was used to assess degradation status considering type, degree and the causative factor based the criteria shown in Table 1. The risks for chemical and physical degradation were calculated as follows:

$$\text{Degradation risk} = Cr * Sr * Tr$$

Where Cr is the climatic rating, Sr is the soil rating and Tr is the topographic rating.

The Cr for chemical degradation was calculated as follows:

$$Cr = PET / (Pa + Q) * 10$$

Where PET is the potential evapotranspiration (mm year^{-1}), Pa is the annual precipitation (mm) and Q is the amount of irrigation water used (mm).

The Cr for physical degradation was calculated as follows:

$$Cr = \Sigma\, Pm^2 / Pa$$

Where Pm is the monthly precipitation (mm) and Pa is annual precipitation (mm).

Table 1. Criteria used to determine the degree of different degradation types

Criteria/Hazard type	Indicator	Unit	Hazard class				
			None	Slight	Moderate	Severe	Extreme
Salinization	EC	dS m^{-1}	< 4	4 - 8	8 - 16	16 - 32	> 32
Sodification	ESP	%	< 10	10 - 15	15 - 30	30 - 50	> 50
Compaction	Bulk density	Mg m^{-3}	< 1.2	1.2 - 1.4	1.4 - 1.6	1.6 - 1.8	> 1.8
Waterlogging	Water table depth	cm	> 150	150 - 100	100 - 50	50 - 30	< 30

The Sr expresses the soil texture rating. In case of chemical degradation, the Sr was 1.5, 1.0 and 0.10 for fine, medium and coarse texture, respectively. For physical degradation, the Sr was calculated as follows:

$$Sr = \text{Silt (\%)} / \text{Clay (\%)}$$

The Tr is reflects the effect of slope, which is usually set as 1.0 when slope values is less than 2% for both chemical and physical degradation risks. Classes of degradation risks are low (risk < 2), moderate (risk = 2-4), high (risk = 4-6) and very high (risk > 6).

Assessment of land productivity index (LPI)

This was done using the revised Storie index (O'geen *et al*., 2008), considering (i) factor A, soil profile depth, (ii) factor B, surface soil texture, (iii) factor C, slope, and (iv) factor X, other properties (drainage, alkalinity, fertility and micro-relief). The calculation is run using Visual Basic application under Microsoft Excel using the following equation:

$$\textbf{Storie index rating} = \frac{A}{100} \times \frac{B}{100} \times \frac{C}{100} \times \frac{X}{100}$$

The productivity grades are arranged in five classes as shown in Table 2.

Assessment of land capability index (LCI)

This was done using the ASLE software (Ismail *et al*., 2001). Parameters included are clay content, available water content, hydraulic conductivity, profile depth, landform, level surface, slope, pH, calcium carbonate content, gypsum content, cation exchange capacity (CEC), exchangeable sodium percentage (ESP), and electrical conductivity (EC). Capability classes are arranged in six classes (Table 2).

Table 2. Productivity grades of Stori index and capability classes of ASLE software

Storie index rating			ASLE software		
Grade	**Description**	**LPI**	**Class**	**Description**	**LCI**
1	Excellent	> 80	1	Excellent	> 80
2	Good	79 - 60	2	Good	79 - 60
3	Fair	59 - 40	3	Fair	59 - 40
4	Poor	39 - 20	4	Poor	39 - 20
5	Non-agricultural	< 20	5	Very poor	19 - 10
			6	Non-agricultural	< 10

Predicting land productivity and land capability

Pedotransfer functions (PTFs) or multiple linear regression (MLR) models were implemented to predict LPI and LCI based on LDF (EC, ESP. bulk density, depth, slope, silt, and clay). Correlation coefficient and root mean square error (RMSE) were used to verify the reliability of models.

Statistical and spatial analysis

Statistical analysis was done using IBM SPSS 19.0 and Microsoft Excel software. The spatial analysis was executed using ArcGIS 10.2.2 software based on the Inverse Distance Weighting (IDW) method, the most common interpolating methods in agriculture practices.

RESULTS AND DISCUSSION

Geomorphology and soils of the area

The main landscape in the area is flood plain. The included landforms (Fig. 2 and Table 3) are levee, overflow mantle, recent terraces, middle terraces and old terraces, representing 8.58, 26.30, 21.01, 35.91 and 8.18% of the total area, respectively. According to Soil Survey Staff (2014a), the soils belong to four subgroups, i.e. (i) Typic Torrifluvents (Profile No. 2, 5, 7, 8, 13, 15, 16, 17 and 18), (ii) Typic Natrargids (Profile No. 6, 10, 11, 12 and 14), (iii) Vertic Torrifluvents (Profile No. 3, 4, 19 and 20), and (iv) Typic Torriorthents (Profile No. 1 and 9).

Table 3. Geomorphic units and soil taxonomy of the studied area

Landform	Area, km^2	Area, %	Profile	Soil Taxonomy
Levee	76.13	8.58	9	*Typic Torriorthents*
			16 and 18	*Typic Torrifluvents*
Overflow mantle	233.30	26.30	10, 11	*Typic Natrargids*
			13, 15	*Typic Torrifluvents*
			19	*Vertic Torrifluvents*
Recent terraces	186.38	21.01	1	*Typic Torriorthents*
			5	*Typic Torrifluvents*
			6	*Typic Natrargids*
Middle terraces	318.59	35.91	3, 20	*Vertic Torrifluvents*
			7, 8 and 17	*Typic Torrifluvents*
			12 and 14	*Typic Natrargids*
Old terraces	72.69	8.19	2	*Typic Torrifluvents*
			4	*Vertic Torrifluvents*

Soil properties

The weighted mean values of main soil properties are shown in Table 4. The soils were very deep with depth of > 150 cm. They were flat to gently sloping, since slope values were <2%. Based on Soil Science Division Staff (2017), the soils were slightly to moderately alkaline and non-saline to moderately saline, since values of pH ranged from 7.36 to 7.99, and EC ranged from 1.35 to 8.46 dS m^{-1}. The CEC was moderate to high (Hazelton and Murphy, 2016), varying from 22.55 to 57.25 cmolc kg^{-1}. The ESP varied from 6.15 to 37.45, indicating slight to high sodicity hazards (FAO, 1988). Soil organic matter was very low to moderate (Hazelton and Murphy, 2016) with a content ranged from 8.83 to 21.60 g kg^{-1}. Calcium carbonate and gypsum contents were low with values of 21.21 to 36.74 g kg^{-1} for the former and 6.25 to 19.37 g kg^{-1} for the latter. Soil texture classes were clay, clay loam, and loam. Soil bulk density (BD) ranged from 1.58 to 1.99 Mg m^{-3}, *i.e.* moderate to very high (Hazelton and Murphy, 2016). Available water content was medium (Hazelton and Murphy, 2016) and varied from 12.01 to 15.10%. Values of hydraulic conductivity (HC) ranged between 0.18 and 0.60 cm hr^{-1}.

Table 4. Main soil properties of the studied area

Profile	Slope, %	Depth, cm	pH *	EC **, dS m^{-1}	CEC, cmolc kg^{-1}	ESP	OM, g kg^{-1}	$CaCO_3$, g kg^{-1}	Gypsum, g kg^{-1}	Sand, %	Silt, %	Clay, %	Texture	BD, Mg m^{-3}	AWC, %	HC, cm hr^{-1}
1	1.40	150	7.48	1.81	28.21	24.16	12.06	29.19	19.37	27.48	40.10	32.42	CL	1.80	14.70	0.37
2	0.32	150	7.81	5.43	24.25	8.25	12.83	24.04	8.92	28.68	43.44	27.88	CL	1.69	15.00	0.51
3	0.14	150	7.73	5.12	33.03	11.87	16.73	21.21	11.98	24.80	37.24	37.96	CL	1.91	14.70	0.34
4	0.28	150	7.76	5.29	37.27	8.07	12.47	23.15	8.86	26.51	30.66	42.83	C	1.67	14.00	0.21
5	1.44	150	7.55	1.93	35.62	23.62	12.36	29.65	8.38	26.95	32.11	40.94	C	1.78	14.00	0.23
6	0.25	150	7.49	8.46	41.03	18.38	18.14	33.33	6.90	23.10	29.74	47.16	C	1.89	13.90	0.23
7	0.09	150	7.57	1.55	25.55	9.90	12.41	27.84	13.42	27.78	42.85	29.37	CL	1.88	15.10	0.48
8	0.27	150	7.59	5.78	33.61	11.89	12.50	29.13	8.74	24.52	36.86	38.63	CL	1.84	14.00	0.26
9	0.60	150	7.71	1.59	37.51	9.15	12.78	26.29	8.54	27.45	29.44	43.12	C	1.84	13.60	0.21
10	0.14	150	7.53	7.56	43.16	16.96	17.43	33.04	6.99	21.99	28.40	49.61	C	1.88	13.90	0.20
11	0.20	150	7.89	1.71	34.12	16.64	17.13	32.47	7.97	35.82	24.96	39.22	CL	1.99	12.70	0.20
12	0.26	150	7.76	7.11	51.89	37.28	18.01	25.11	6.25	21.57	18.79	59.65	C	1.92	12.70	0.18
13	0.00	150	7.45	1.35	57.25	34.00	10.76	35.07	7.58	17.90	16.30	65.80	C	1.87	12.01	0.30
14	0.48	150	7.80	6.13	51.51	37.45	21.60	24.27	8.35	16.20	24.59	59.21	C	1.90	13.70	0.21
15	0.20	150	7.99	1.91	35.67	15.84	16.98	29.24	7.24	32.68	26.32	41.00	C	1.90	14.00	0.20
16	0.09	150	7.74	7.13	32.53	13.03	16.85	32.30	6.75	32.21	30.40	37.39	CL	1.82	13.40	0.24
17	0.25	150	7.71	3.72	22.55	6.15	9.87	29.74	9.37	33.83	40.26	25.92	L	1.58	14.30	0.60
18	0.14	150	7.36	7.43	35.36	10.89	15.69	36.74	8.82	30.68	28.68	40.65	C	1.91	13.60	0.22
19	0.28	150	7.75	6.18	34.43	11.48	15.84	29.75	7.62	26.17	34.26	39.57	C	1.77	14.60	0.32
20	0.39	150	7.74	3.65	36.23	6.78	8.83	29.23	7.60	21.23	37.13	41.64	C	1.70	15.00	0.24

*** 1:2.5 soil : water suspension; ** soil paste extract; EC, electrical conductivity; CEC, cation exchange capacity; ESP, exchangeable sodium percentage; OM, organic matter; C, clay; CL, clay loam; L, loam; BD, bulk density; AWC, available water content; HC, hydraulic conductivity**

Assessment of degradation status

Each of EC, ESP, and BD was considered, while soil depth was not since it was within the safe limit for waterlogging (> 150 cm). The spatial distribution for each of EC, ESP, and BD is shown in Fig. 3 and Table 5. Results illustrate that 39.95% of soils remained within the safe limit for salinization, since EC remained below 4 dS m^{-1}. Soils with slight salinization hazards occupied the majority of the area (59.60%), while those with moderate hazards did not exceed 1% of the total area. The spatial distribution of ESP shows that 6.49% of the soils had no sodification hazards, since their ESP values were below the safe limit of 10. Soils with slight and moderate sodification hazards covered over 90% of the total area, while those with severe hazards dominated the smallest portion (3.16%). Salinization and sodification are two common processes in the Nile Delta region, especially in the northern parts, where about 46% of the soils are salt-affected (Negm, 2017).

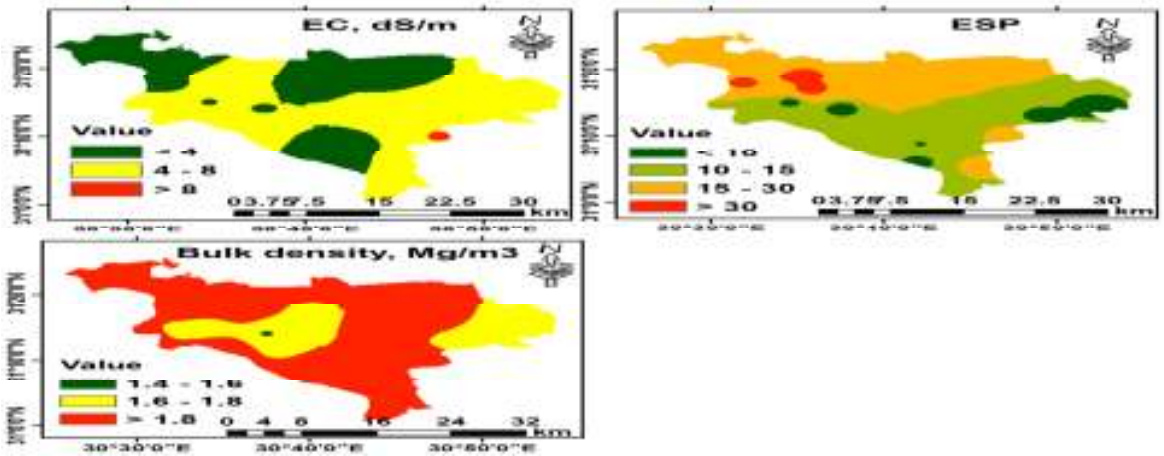

Fig. 3. Spatial distribution of EC, ESP and bulk density (BD) in the studied area

This is due to the Mediterranean seawater intrusion as well as human intervention through poor land and water management practices. These practices include over-irrigation with insufficient drainage, irrigation using low-quality water, poor land leveling, excessive fertilization, lake conservation measures, improper cropping patterns and rotations (Mohamed, 2017a). Soils affected by extreme compaction hazards covered the largest part (74.22%). Soils affected by severe hazards occupied 25.62%, while those affected by moderate hazards represented only < 1%. Soil compaction is caused, on one hand, due to improper time use of heavy machinery (ElBaroudy and Moghanm, 2014). On the other hand, soils of the Nile Delta are fine in texture (heavy clay to clay loam) containing a majority of micro-pores but a minority of macro-pores, and thus they are considered compacted-ready soils, in addition to high BD reaching 1.5 to 1.6 Mg m^{-3} (Mohamed, 2017a).

Table 5. Areas and percentages of degradation hazards in the studied area

Degree	Salinization			sodification			Compaction		
	EC, dS m^{-1}	Area		ESP	Area		BD, Mg m^{-3}	Area	
		km^2	%		km^2	%		km^2	%
None	< 4	354.38	39.95	< 10	57.58	6.49	< 1.2	---	---
Slight	4 - 8	528.73	59.60	10 - 15	399.66	45.05	1.2 – 1.4	---	---
Moderate	8 - 16	3.98	0.45	15 - 30	401.79	45.29	1.4 - 1.6	1.42	0.16
Severe	8 - 16	---	---	30 - 50	28.06	3.16	1.6 - 1.8	227.28	25.62
Extreme	> 16	---	---	> 50	---	---	> 1.8	658.39	74.22

EC, electrical conductivity; ESP, exchangeable sodium percentage; BD, bulk density

Assessment of degradation risk

The natural vulnerability of land degradation was evaluated considering climatic, topographic and soil (depth and texture) factors. The slope gradient had an insignificant effect, since it was less than 2%, and thus the topographic effect was set as 1.0. The obtained results (Fig. 4) indicate a chemical risk not exceeding 1.0, indicating low risk. On the other hand, the area was affected by moderate to very high physical degradation risk since the risk values ranged from 2.94 to 18.53. Soils affected by very high risk covered 849.75 km^2, representing 95.79% of the area. Soils affected by high and moderate risks occupied 32.96 and 4.38 km^2, representing 3.72 and 0.49% of the total area, respectively. The irregular rainfall distribution during the year is the main factor for physical risks.

Land evaluation for agricultural use

The spatial distribution of LPI (Fig. 5) shows that the productivity classes in the area ranged between good (Grade 2) and poor (Grade 4), since the LPI varied from 20.09 to 72.92. Soils of fair productivity (Grade 3) covered 58.69% of the area, and soils of poor productivity (Grade 4) represented 37.39%, while soils of good productivity (Grade 2) occupied the smallest portion (3.92%). On the other hand, the spatial distribution of LCI (Fig. 8) indicates that soils belonged to two capability classes; Class 2 (Good) and Class 3 (Fair), since the LCI ranged from 47.77 to 76.90. About two-thirds of the soils (600.58 km^2) belonged to Class 2, while the remaining area (286.51 km^2) belonged to Class 3.

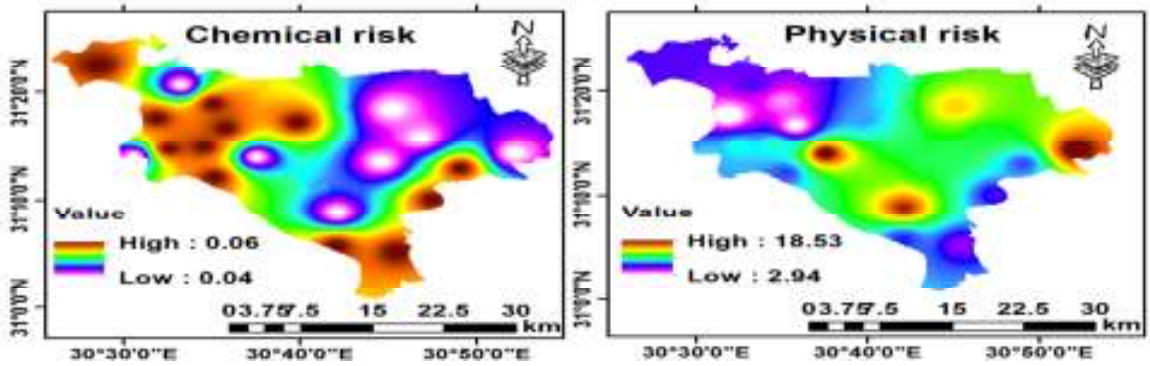

Fig. 4. Degradation risks in the studied area

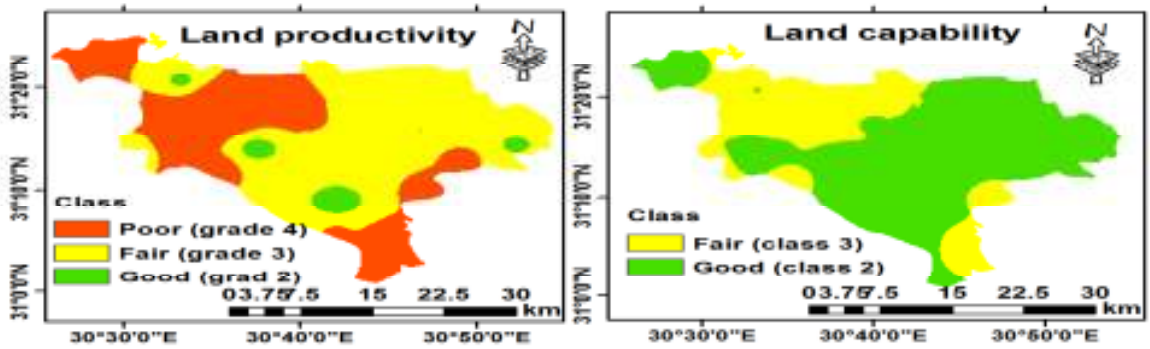

Fig. 5. Spatial distribution of LPI and LCI in the studied area

Pearson's correlation (Table 6) show significant positive correlation ($P < 0.05$) between LPI and LCI. Thus, the two systems for land evaluation showed a similar trend, and they are close to appraise soils of the studied area with regard to the agricultural utilization. Sayed *et al.* (2016) reported that the revised Storie index and ASLE software showed similar prediction trend when evaluating soils representing western limestone plateau in Assiut governorate.In view of using the two systems for land evaluation, the main limiting factors are soil texture, salinity, and sodicity. Although fine texture is favorable for fertility status and water retention, it restricts water infiltration, especially in heavy soils. Thus, salt accumulation poses potential problems that require precise management practices. Such practices include intermittent leaching, adequate drainage, frequent application of

leaching fraction (10-20%), furrow irrigation, addition of organic and chemical amendments and selecting salt-tolerant crops (Mohamed, 2017b).

Predicting land's agricultural potentiality based on LDF

The PTFs or MLR models were implemented considering EC, ESP, BD, silt, and clay, while slope and depth were excluded since they remained within the safe limits for degradation.

(1) Predicting land productivity

There was a significant negative correlation ($P < 0.05$) between LPI and ESP (Table 6). The LPI showed a highly significant positive correlation ($P < 0.01$) with silt content, but a highly significant negative correlation ($P < 0.01$) with clay content. On the other hand, the LPI showed no significant correlations with EC and BD. Consequently, ESP, silt, and clay were used for predicting the LPI. The MLR model resulted in the following equation:

LPI = 114.049 + 0.452 ESP – 0.120 Silt – 1.79 Clay ---- (1)

A prediction of the LPI was performed considering the five factors, and the MLR model resulted in the following equation:

LPI = 27.945 – 1.569 EC + 0.212 ESP + 35.146 BD + 0.373 Silt – 1.378 Clay ----- (2)

Table 6. Correlation matrix between LDF and land indices

	EC	ESP	BD	Silt	Clay	LCI	LPI
EC	1.000	0.010	0.045	-0.089	0.186	-0.273	-0.365
ESP	0.010	1.000	0.471*	-0.680**	0.775**	-0.854**	-0.519*
BD	0.045	0.471*	1.000	-0.552*	0.448*	-0.500*	-0.208
Silt	-0.089	-0.680**	-0.552*	1.000	-0.881**	0.773**	0.692**
Clay	0.186	0.775**	0.448*	-0.881**	1.000	-0.824**	-0.797**
LCI	-0.273	-0.854**	-0.500*	0.773**	-0.824**	1.000	0.544*
LPI	-0.365	-0.519*	-0.208	0.692**	-0.797**	0.544*	1.000

*** Correlation is significant at the 0.05 level; ** Correlation is significant at the 0.01 level; EC, electrical conductivity; ESP, exchangeable sodium percentage; BD, bulk density; LCI, land capability index; LPI, land productivity index**

The analysis of variance (ANOVA) for prediction the LPI showed that the two models were a suitable fit for the data (Table 7). Results of verification (Fig. 6) show that values of the correlation coefficient (r) and root mean square error (RMSE) were 0.81** and 10.47, respectively for model 1, and 0.85** and 9.51, respectively for model 2. This indicates that predicting the LPI using model 2 gave the best results.

(2) Predicting land capability

There was a significant negative correlation ($P < 0.05$) between LCI and BD. Moreover, the LCI had a high positive correlation ($P < 0.01$) with silt, but high negative correlations with ESP and clay. On the other hand, there was a non-significant correlation between LCI and EC. Predicting the LCI using the correlated parameters, the MLR model resulted in the following equation:

LCI = 70.506 – 0.302 ESP – 2.677 BD + 0.142 Silt – 0.125 Clay ----- (3)

A prediction of the LCI using the five factors resulted in the following equation:

LCI = 65.529 – 0.535 EC – 0.350 ESP – 1.504 BD + 0.211 Silt – 0.026 Clay ----- (4)

The ANOVA for prediction the LCI showed that the two models were a good fit for the data (Table 8). Results of verification (Fig. 7) show that values of r and RMSE were 0.898 and 2.476, respectively for model 3, and 0.924 and 2.149, respectively for model 4. This indicates that predicting the LCI using model 4 gave the best results.

Table 7. Analysis of variance for the LPI prediction

	Sum of Squares	df	Mean Square	F value	Significance
Model 1					
Regression	4037.183	3	1345.728	10.343	0.001
Residual	2081.697	16	130.106		
Total	6118.880	19			
Model 2					
Regression	4399.736	5	879.947	7.166	0.002
Residual	1719.144	14	122.796		
Total	6118.880	19			

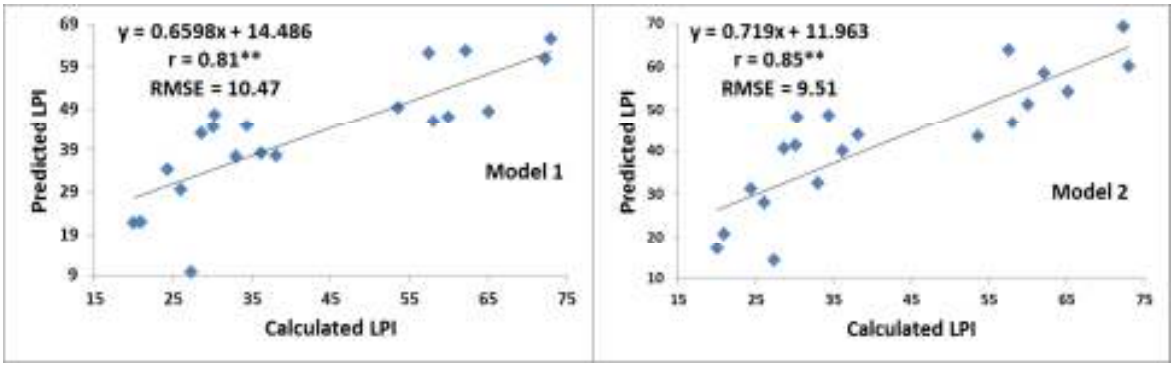

Fig. 6. Comparison of predicted and calculated LPI using the two models

Table 8. Analysis of variance for the LCI prediction

	Model 3				
	Sum of Squares	**df**	**Mean Square**	**F value**	**Significance**
Regression	486.618	4	121.654	15.662	0.000
Residual	116.515	15	7.768		
Total	603.133	19			
	Model 4				
Regression	515.397	5	103.079	16.448	0.000
Residual	87.736	14	6.267		
Total	603.133	19			

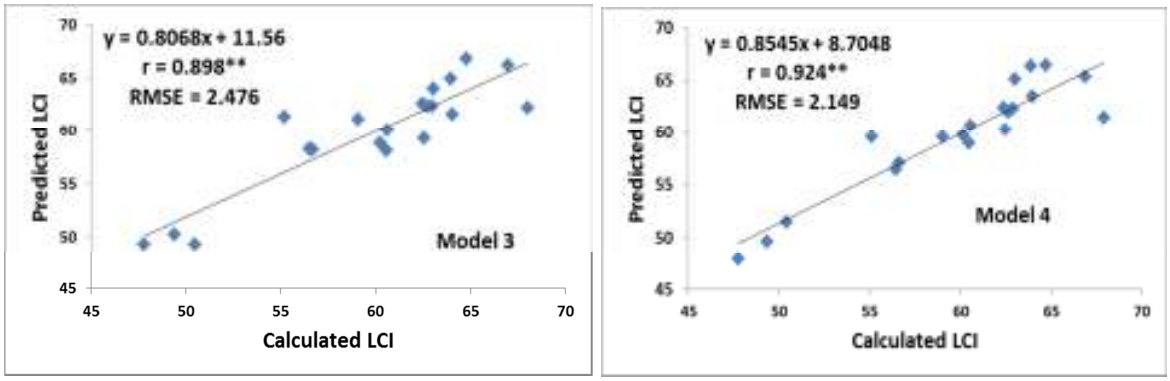

Fig. 7. Comparison of predicted and calculated LCI using the two models

CONCLUSION

The area was affected by salinity, sodicity, and compaction hazards, while water logging remained within the safe limit. Main factors involved in such hazards related to seawater intrusion by the Mediterranean Sea and improper soil, water, and crop management practices. Chemical degradation risks were low, while moderate to very high physical degradation risks dominated the area. The revised Stori index showed that the area belonged to three productivity grades, *i.e.* good (grade 2), fair (grade 3), and poor (grade 4). The ASLE software indicated two capability classes; good (class 2) and fair (class 3). The two systems showed close results, indicating a similar trend in land evaluation. The multiple linear regression models showed that predicting the LPI and LCI based on EC, ESP, bulk density, silt, and clay resulted in high reliability and a good fit for the data. These models can provide valuable tools to monitor land performance to achieve sustainable development.

ACKNOWLEDGMENT

The authors express their deep thanks to prof. Dr. Ali Ahmed Abdelsalm, Soil and Water Department, Faculty of Agriculture, Benha University, Egypt and Prof. Dr. Mahmoud Khairy, Soil, Water and Environment, Research Institute, Agricultural Research Center, Egypt, for their valuable comments.

REFERENCES

Abdel Meguid, M. (2017). Key features of the Egypt's water and agricultural resources. In: Negm, A.M. (Ed.), Conventional water resources and agriculture in Egypt. Springer Berlin Heidelberg, Germany, pp. 1-61.

AbdelRahman, M.A.E., Shalaby, A., Aboelsoud, M.H., Moghanm, F.S. (2017). GIS spatial model based for determining actual land degradation status in Kafr El-Sheikh Governorate, North Nile Delta. *Mod. Earth Sys. Environ.* (In Press).

Blume, H.P., Brümmer, G.W., Fleige, H., Horn, R., Kandeler, E., Kögel-Knabner, I., Kretzschmar, R., Stahr, K., Wilke, B.-M. (2016). Land evaluation and soil protection. In: Blume, H.-P., Brümmer, G.W., Fleige, H., Horn, R., Kandeler, E., Kögel-Knabner, I., Kretzschmar, R., Stahr, K., Wilke, B.-M. (Eds.), Scheffer/SchachtschabelSoil Science. Springer Berlin Heidelberg,, Germany, pp. 561-585.

D'Odorico, P., Bhattachan, A., Davis, K.F., Ravi, S., Runyan, C.W. (2013). Global desertification: Drivers and feedbacks. *Adv. Water Resour.* 51, 326–344.

ElBaroudy, A.A., Moghanm, F.S. (2014). Combined use of remote sensing and GIS for degradation risk assessment in some soils of the Northern Nile Delta, Egypt. *Egypt. J. Rem. Sens. Space Sci.* 17, 77-85.

EMA (2011). The normals for Sakha station, (1960 – 2010). Egyptian Meteorological Authority (EMA). Ministry of Civil Aviation, Cairo, Egypt.

Embabi, N.S. (2018). The Nile Delta. In: Embabi, N.S. (Ed.), Landscapes and landforms of Egypt: Landforms and evolution. Springer International Publishing, Cham, pp. 57-68.

FAO (1980). A provisional methodology for soil degradation assessment. FAO, Rome, Italy.

FAO (1988). Salt-affected soils and their management. FAO Soils Bulletin No. 39. FAO, Rome, Italy.

FAO (2006). Guidelines for soil description. FAO, Rome, Italy.

Hazelton, P., Murphy, B. (2016). Interpreting soil test results: what do all the numbers mean? CSIRO publishing, Collingwood Victoria, Australia.

Ismail, H.A., Morsy, I.M., EL-Zahaby, E.M., El-Nagar, F.S. (2001). A Developed Expert System for land use planning by coupling Land Information System (LIS) and Modeling. *Alex. J. Agric. Res.* 46, 141-154.

Mahala, A. (2017). Processes and status of land degradation in a plateau fringe region of tropical environment. *Environ. Process.* 4, 663-682.

Mganga, K.Z., Nyariki, D.M., Musimba, N.K.R., Amwata, D.A. (2018). Determinants and rates of land degradation: Application of stationary time-series model to data from a semi-arid environment in Kenya. *J. Arid Land* 10, 1-11.

Mohamed, N.N. (2017a). Land degradation in the Nile Delta. In: Negm, A.M. (Ed.), The Nile Delta. Springer International Publishing, Cham, pp. 235-264.

Mohamed, N.N. (2017b). Management of salt-affected soils in the Nile Delta. In: Negm, A.M. (Ed.), The Nile Delta. Springer International Publishing, Cham, pp. 265-295.

Negm, A.M. (2017). The Nile Delta: Update, conclusions, and recommendations. In: Negm, A.M. (Ed.), The Nile Delta. Springer International Publishing, Cham, pp. 519-530.

O'geen, A.T., Southard, S.B., Southard, R.J. (2008). A revised Stori index for use with digital soil information Regents of the University of California Agricultural and Natural Resources, Publication, USA.

Ravi, S., Breshears, D.D., Huxman, T.E., D'Odorico, P. (2010). Land degradation in drylands: Interactions among hydrologic-aeolian erosion and vegetation dynamics. *Geomorphology* 116, 236-245.

Safriel, U. (2017). Land degradation neutrality (LDN) in drylands and beyond - where has it come from and where does it go. *Silva Fenn.* 51, 1-19.

Said, A., Zohry, A.E., Ouda, S. (2016). Unconventional solution to increase water and land productivity under water scarcity. Major crops and water scarcity in Egypt: Irrigation water management under changing climate. Springer International Publishing, Cham, pp. 99-115.

Sayed, Y.A., El-Desoky, M.A., Gameh, M.A., Faragallah, M.A. (2016). Land capability of some soils representing western limestone Plateau at Assiut. *Assiut J. Agric. Sci.* 47, 120-141.

Soil Science Division Staff (2017). Soil survey manual. USDA Handbook 18. Government Printing Office, Washington, D.C, USA.

Soil Survey Staff (2014a). Keys to soil taxonomy. USDA-Natural Resources Conservation Service, Washington, DC, USA.

Soil Survey Staff (2014b). Soil survey field and laboratory methods manual. Soil Survey Investigations Report No. 51, Version 2.0. R. Burt and Soil Survey Staff (ed.). U.S. Department of Agriculture, Natural Resources Conservation Service, Washington, DC.

Zinck, J.A., Valenzuela, C.R. (1990). Soil geographic database: structure and application examples. *ITC Journal* 3, 270-294.

Zohry, A., Ouda, S.A. (2018). Prevailing cropping pattern. In: Ouda, S.A.H., Zohry, A.E.-H., Morsy, M. (Eds.), Cropping pattern modification to overcome abiotic stresses : Water, salinity and climate. Springer International Publishing, Cham, pp. 21-35.

التنبؤ بإمكانية الزراعة بإستخدام عوامل تدهور الأرض في شرق فرع رشيد - دلتا النيل - مصر

أحمد سعيد أبوزيد[١] ، محمد احمد بسيوني[١]و عبداللطيف دياب عبداللطيف[٢]

[١]قسم الأراضي والمياه - كلية الزراعة - جامعة بنها – مصر

[٢]معهد بحوث الأراضي والمياه والبيئة – مركز البحوث الزراعية – مصر

يهدف هذا البحث إلى التنبؤ تأثير عوامل تدهور الأراضي على إمكانية الزراعة في بعض المناطق الواقعة بمحافظة كفر الشيخ بشرق نهر النيل (فرع رشيد). ولتحقيق ذلك تم تمثيل الوحدات الجيومورفولوجية بالمنطقة بعدد ٢٠ قطاع أرضي جمعت منها عينات التربة وتم تحليل خواصها الكيميائية والفيزيائية. أظهرت النتائج أن المنطقة تعاني من مشاكل الملوحة، الصودية، الإنضغاط، بينما لم تظهر مشاكل متعلقة بالغدق المائي حيث أن عمق التربة يزيد عن ١٥٠ سم. وجد ان أهم عوامل التدهور هي تداخل مياه البحر المتوسط، وسوء إدارة التربة والمياه. وجد ان أخطار التدهور الكيميائي كانت منخفضة، بينما كانت أخطار التدهور الفيزيائي كانت متوسطة إلى عالية جداً. تراوحت إنتاجية التربة ما بين جيده (درجة ثانية) إلى فقيرة (درجة رابعة)، في حين كانت قدرة التربة جيدة (درجة ثانية) إلى متوسطة (درجة ثالثة). أوضحت نتائج الإنحدار الخطي المتعدد دقة أعلى عند التنبؤ بمعامل الإنتاجية ومعامل القدرة على أساس التوصيل الكهربي، نسبة الصوديوم المتبادل، الكثافة الظاهرية، نسبة السلت، ونسبة الطين.